REPORT DOCUMENTATION PAGE

AFRL-SR-AR-TR-05-

0047

1. REPORT DATE (DD-MM-YYYY)	2. REPORT TYPE	3. DATES COVERED (From - To)
02-02-2005	Final	15 Dec 03 - 14 Dec 04

4. TITLE AND SUBTITLE
Characterization of Instrument Effects in Imaging and Non-Imaging Polarimeters

5a. CONTRACT NUMBER

5b. GRANT NUMBER
FA9550-04-1-0025

5c. PROGRAM ELEMENT NUMBER

6. AUTHOR(S)
J. Scott Tyo

5d. PROJECT NUMBER

5e. TASK NUMBER

5f. WORK UNIT NUMBER

7. PERFORMING ORGANIZATION NAME(S) AND ADDRESS(ES)
University of New Mexico
Scholes Hall
Albuquerque, NM 87131

8. PERFORMING ORGANIZATION REPORT NUMBER
N/A

9. SPONSORING/MONITORING AGENCY NAME(S) AND ADDRESS(ES)
Dr. Kent Miller
AFOSR/NE
801 N. Randolph St, Room 732
Arlington, VA 22203

10. SPONSOR/MONITOR'S ACRONYM(S)

11. SPONSOR/MONITOR'S REPORT NUMBER(S)

12. DISTRIBUTION/AVAILABILITY STATEMENT
Unlimited

DISTRIBUTION STATEMENT A
Approved for Public Release
Distribution Unlimited

20050218 051

13. SUPPLEMENTARY NOTES

14. ABSTRACT

The purpose of this one-year effort was to identify and investigate some important effects that the optical systems have on the performance of imaging and non-imaging polarimeters. During our period of performance we concentrated on two primary areas: 1) Characterization of the effects of systematic errors in the polarization optics of non-imaging polarimeters through measurements and comparing these results to previous theory; and 2) Investigation of the effects of focal plane array nonuniformity on the performance of imaging polarimeters. In the first area, we have made some of the only available measurements that demonstrate the theoretical predictions made over the past several years. We have build a manually operated polarimeter testbed system, and are in the process of building a fully automated polarimeter testbed system. In the second area, we have modeled a rotating-retarder polarimeter operating with a focal plane array exhibiting response nonuniformity. We have found that gain and bias nonuniformity affect the imagery differently, and can be mitigated using NUC techniques that have been developed for conventional IR imagery.

15. SUBJECT TERMS
Remote Sensing, Polarization, Infrared Imaging

16. SECURITY CLASSIFICATION OF:			17. LIMITATION OF ABSTRACT	18. NUMBER OF PAGES	19a. NAME OF RESPONSIBLE PERSON
a. REPORT	b. ABSTRACT	c. THIS PAGE			J. Scott Tyo
U	U	U	UU	21	19b. TELEPHONE NUMBER (Include area code) 505-277-1412

Final Technical Report

Characterizaiton of Instrument Effects in Imaging and Non-Imaging Polarimeters

Award Number: FA9550-04-1-0025
December 15, 2003 – December 14, 2004

Submitted to:
Dr. Kent Miller
AFOSR/NE
801 N. Randolph St, Room 732
Arlington, VA 22203

PI: J. Scott Tyo
Electrical and Computer Engineering Department
University of New Mexico
Albuquerque, NM 87131-1356 USA
tyo@ieee.org

ABSTRACT

The purpose of this one-year effort was to identify and investigate some important effects that the optical systems have on the performance of imaging and non-imaging polarimeters. During our period of performance we concentrated on two primary areas: 1) Characterization of the effects of systematic errors in the polarization optics of non-imaging polarimeters through measurements and comparing these results to previous theory; and 2) Investigation of the effects of focal plane array nonuniformity on the performance of imaging polarimeters. In the first area, we have made some of the only available measurements that demonstrate the theoretical predictions made over the past several years. We have build a manually operated polarimeter testbed system, and are in the process of building a fully automated polarimeter testbed system. One of the most important results presented in this report shows the balance between the effects of systematic error and the effects of noise in the reconstructed Stokes parameters. In the second area, we have modeled a rotating-retarder polarimeter operating with a focal plane array exhibiting response nonuniformity. We have found that gain and bias nonuniformity affect the imagery differently, and can be mitigated using nonuniformity correction techniques that have been developed for conventional IR imagers.

1. INTRODUCTION

1.1. Motivation

The measurement and exploitation of polarization information has become a high priority in a variety of Air Force and DoD remote sensing missions. Polarization provides a useful dimension of information that helps to characterize shape and surface characteristics of interesting targets in optical imagery from the UV through the LWIR and beyond. Polarization has been shown to be useful for target detection[1] and identification,[2] machine vision,[3] and remote sensing,[4] and has been shown to help defeat clutter[5] and mitigate the effect of random media.[1,6]

While it is clear that polarization can be a potentially powerful tool, it is of paramount importance to mitigate the effects of noise and errors. In many cases, the signal that is being sought is on the order of 1% degree of polarization. When this is the case, noise either from the detector or from systematic errors in the collection of the data can be enough to prevent the detection of the signal.

In recent years, there has been significant investigation of ways to optimize both passive (Stokes) and active (Mueller) polarimeters in the presence of noise. The majority of studies have focused on the effects of additive noise at the receiver.[7–10] When this type of noise is dominant, the condition number of the processing matrices must be minimized for an optimum system. A handful of other studies have attempted to quantify the error when the noise is due to systematic effects, such as inaccuracies in the angles or retardances of the polarization optics,[11,12] misalignment between successive measurements,[13] and focal plane nonuniformity.

In this program we undertook research designed to identify and characterize the sources and effects of such errors in both imaging and non-imaging polarimeters. The primary areas of research in this program were aimed at

- Developing a polarimeter testbed system
- Understanding the effect that various instrumental errors have on non-imaging polarimeter performance and identify the most important problems for further study
- Studying the interaction between instrumental errors and scene variability in order to understand how errors will affect the *exploitation* of polarization imagery
- Investigating the effects of focal plane array nonuniformity on the performance of imaging polarimeters.

The results of these studies provide significant information about the design of polarimetric remote sensing instruments. If there is a good understanding of the nature and magnitude of the errors in polarimeters, greater care can be exercised in the design of devices in a variety of remote sensing circumstances.

1.2. Background and General Optimization

Most imaging optical polarimeters rely on a series of intensity measurements to reconstruct the Stokes vector. While the stokes vector can be written

$$\mathbf{S} = \begin{bmatrix} <|E_x|^2> + <|E_y|^2> \\ <|E_x|^2> - <|E_y|^2> \\ <|E_{45}|^2> - <|E_{-45}|^2> \\ <|E_{lcp}|^2> - <|E_{rcp}|^2> \end{bmatrix}, \tag{1}$$

usually intensity measurements are not made at the six settings indicated in (1) (horizontal linear (x), vertical linear (y), $\pm 45°$ linear, and left- and right circular polarization). The polarimeter is usually composed of a series of retarders and analyzers that can be individually controlled[1]. The Mueller matrices of these optics can be cascaded into a single system Mueller matrix for the i^{th} realization of the system $\underline{\underline{\mathbf{M}}}_i$. The input and output Stokes vectors are related by

$$\mathbf{S}_{out,i} = \underline{\underline{\mathbf{M}}}_i \cdot \mathbf{S}_{in}. \tag{2}$$

Since the detector in the polarimeter measures only the intensity of the output Stokes vector (s_0), we can relate a series of intensity measurements to the input Stokes vector as

$$\mathbf{I} = \underline{\underline{\mathbf{A}}} \cdot \mathbf{S}_{in}, \tag{3}$$

where $\mathbf{I}$ is the vector of intensity measurements and the i^{th} row of $\underline{\underline{\mathbf{A}}}$ is the first row of $\underline{\underline{\mathbf{M}}}_i$. When the input Stokes vectors are uniformly distributed over the Poincarè sphere, the SNR is optimized by minimizing the condition number of $\underline{\underline{\mathbf{A}}}$, then inverting the matrix and estimating the unknown input Stokes vector as

$$\hat{\mathbf{S}}_{in} = \underline{\underline{\mathbf{A}}}^{-1} \cdot \mathbf{I}. \tag{4}$$

The study of polarization error can be reduced to characterizing the Stokes vector error

$$\varepsilon = \hat{\mathbf{S}} - \mathbf{S} \tag{5}$$

as a function of the parameters of the system.

2. DEVELOPMENT OF THE POLARIMETER TESTBED

2.1. Manual System

In the first several months of the AFOSR effort that commenced in December 2003, the PI developed a polarimeter testbed in the Multi Dimensional Imagery Lab (MDIL) at UNM. A schematic of the testbed is shown in fig. 1. The polarimeter testbed is used to measure statistical properties of polarimeters by changing the parameters of the system. The testbed has an active source (a HeNe laser operating at 633 nm) and various fixed and variable retarders (several Meadowlark Optics Liquid Crystal Variable Retarders). Currently the testbed is operated manually in a nonimaging mode, but we will endeavor to upgrade it to a fully automatic, fully imaging testbed under this program and an accompanying DURIP proposal that will be submitted later this year. Examples of measurements made in the MDIL under the current AFOSR program are shown below.

[1]For example, rotating retarder systems spin a retarder in front of an analyzer, and variable retardance systems have two static, tunable retarders in front of an analyzer.

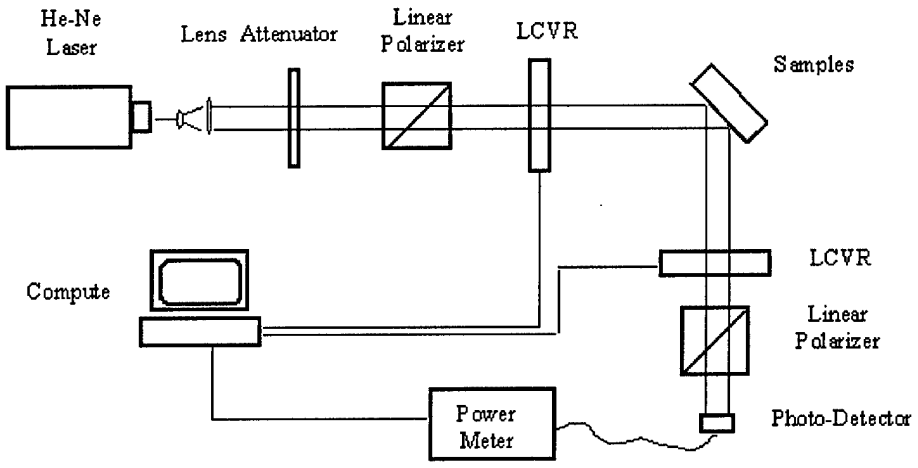

Figure 1. Layout of the polarimeter testbed in the MDIL at UNM. The testbed is configured to study the effects of retarder positioning error in this photograph.

Figure 2. Layout of the automated polarimeter testbed system currently under development.

2.2. Automated System

In order to make the experimental process more efficient and accurate, we are working on designing an automated system with which to conduct these characterization experiments. The main task in converting the manual system to an automatic system is devising a method to control the rotating elements and variable retarders from the computer. We have chosen New Focus Model 8401 Motorized Rotary Stage for mounting the polarizer. The model 8401 Motorized Rotary Stage is an open-loop automatic rotary stage with a resolution better than 0.2 mrad. The New Focus Intelligent Driver Model 8753 is used to control the Model 8401 Motorized Rotary Stage. The Intelligent Driver Model 8753 is connected with the computer. DLL commands are used for communication between the computer and driver model. The automatic system is shown in fig. 2 The automated testbed system is currently a work in progress. Work will continue on the automated testbed under out recently begun award # FA9550-05-1-0090.

3. CHARACTERIZING DIFFERENT ERROR SOURCES IN NON-IMAGING POLARIMETERS

The PI has been actively involved in the development, calibration, and optimization of imaging and non-imaging polarimeters. His work includes a current AFOSR sponsored program that began in 2003, to study instrument effects in polarimeters. This section briefly reviews the prior work by the PI and his colleagues relavent to the current proposal.

One of the first important contributions to the field was the understanding of the role of polarimeter design on the observed SNR in reconstructed Stokes images. Until very recently, polarimeters were designed to operate in a suboptimal fashion that artificially lowered the SNR for a given detector SNR.

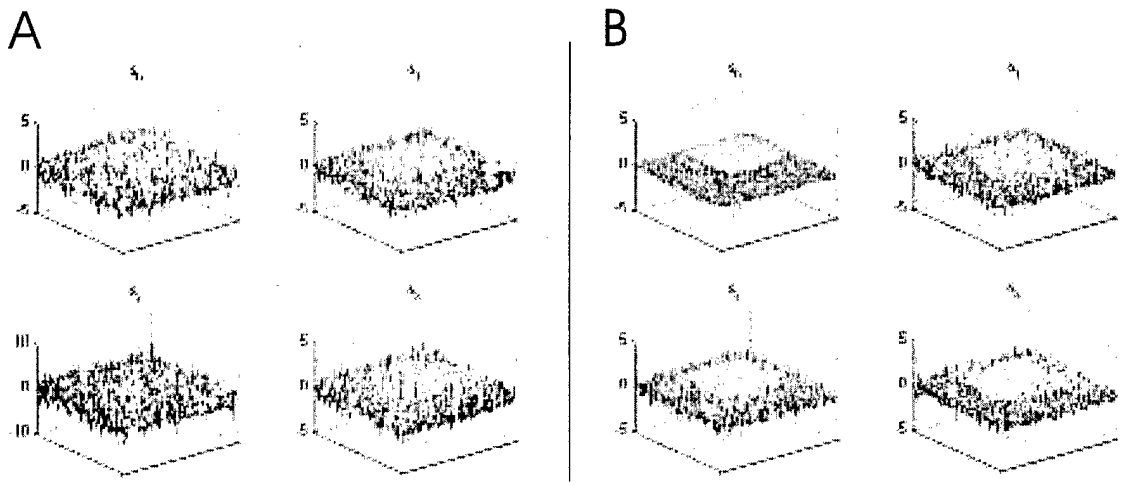

Figure 3. Demonstration of the effect of optimizing condition number. The left panel was simulated with a non-optimized variable retardance system. The right panel was simulated with an optimum system.

The key to understanding the role of polarimeter design on SNR lies in (4). When there is a small noise component to the intensity measurement, the noise is transformed by the inverse matrix $\underline{\underline{\mathbf{A}}}^{-1}$. The length of the transformed noise vector is globally minimized by optimizing the condition number of the system matrix $\underline{\underline{\mathbf{A}}}$. Performing such an optimization can raise the SNR in reconstructed Stokes vector images by 10 dB or more. These results were derived and explained by the PI and others for rotating retarder[8,11] and variable retardance[9,11] Stokes vector polarimeters.

All of the theory developed to date has assumed that the input Stokes vector is uniformly distributed over the Poincarè sphere. However, in many remote sensing applications, the input Stokes vector is not uniformly distributed. For example, there are scenarios when the dominant polarization signal will be positive in the s_1 channel[2]. In this case, the choice of optimum parameters will be different in order to maximize SNR in that channel. Recently, researchers in collaboration between AFRL and UNM have obtained results indicating that the direction of the error – not just the magnitude – also depends on the input polarization state. Understanding of these phenomena will help to develop more accurate polarimeters for particular applications.

3.1. Numerical Modeling of Systematic Errors

In contrast to noise and SNR, which are properties of the detector and the signal to be measured, systematic errors include issues such as positioning error for optical elements, calibration errors, and spatial nonuniformity. In many cases, the effects of systematic errors are more detrimental to the final Stokes parameter images than noise introduced in the detection process. For example, in a rotating retarder polarimeter, a retarder (often a quarter wave plate) is rotated to at least four discrete

[2]An example of this is when the scene being imaged is largely flat, and the wavelengths are in the reflective regime, i.e. visible wavelengths over a flat earth.

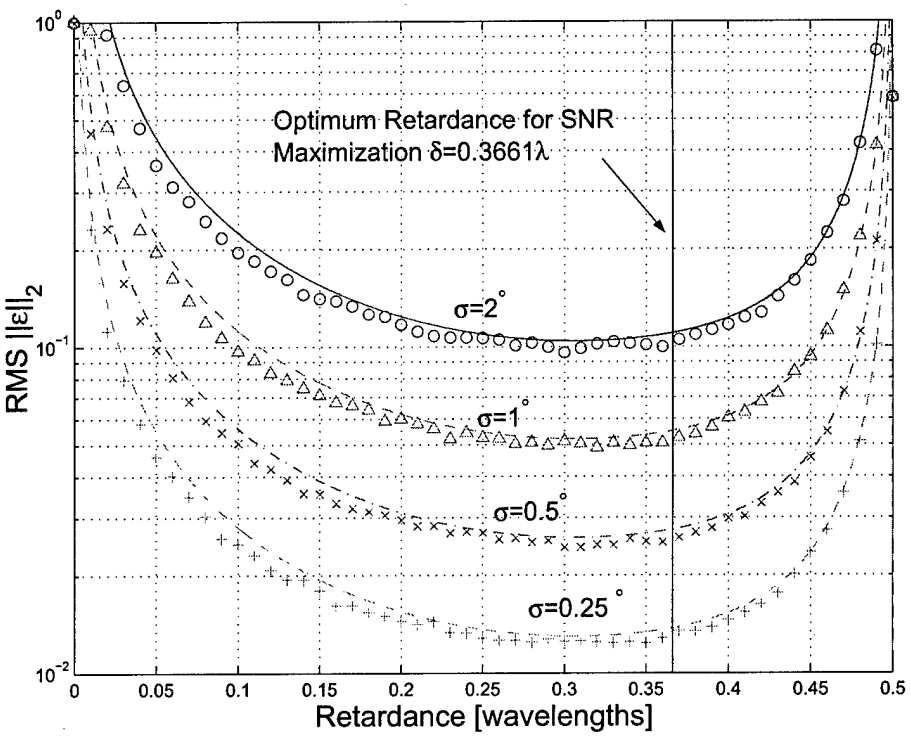

Figure 4. Mean squared error of a rotating compensator Stokes vector polarimeter as a function of retardance. These data were all obtained at the near optimal angles of $\pm 15.1, \pm 51.6$. In each trace, angular positioning error with standard deviation as given was assumed. The solid lines represent theoretical predictions. The data points are simulation.

angles in front of a fixed analyzer. If there are errors in the positioning of the retarder, this can have an effect on the reconstructed Stokes vector at each pixel in a scene. Similarly, retarders often have spatially nonuniform retardance. This affects the assumption of the ideal nature of the retarders used in forming the processing matrices and leads to errors in reconstructed Stokes vector images. The PI has developed a general theoretical framework describing these phenomena in Stokes vector imagers.[11] Those results show how to minimize systematic errors. Fig. 4 presents a plot of the mean squared error in Stokes vector polarimeters assuming uniformly distributed input polarization states. Fig. 4 clearly identifies the optimum retardance for minimizing the effects of systematic errors.

3.2. Effect of Input State on Error

Just as discussed in section 2 for SNR, the actual effect of instrument errors will be dependent on the input polarization state. Fig. 5 shows average error in reconstructing a Stokes vector as a function of location of the input polarization state on the Poincarè sphere. These results are for a rotating retarder Stokes vector polarimeter that has been optimized to minimize the average error over all possible incident states. Note that the minimum error is less than half the maximum error. This figure clearly demonstrates that one can improve performance of the polarimeter if there is knowledge of the expected input polarization state.

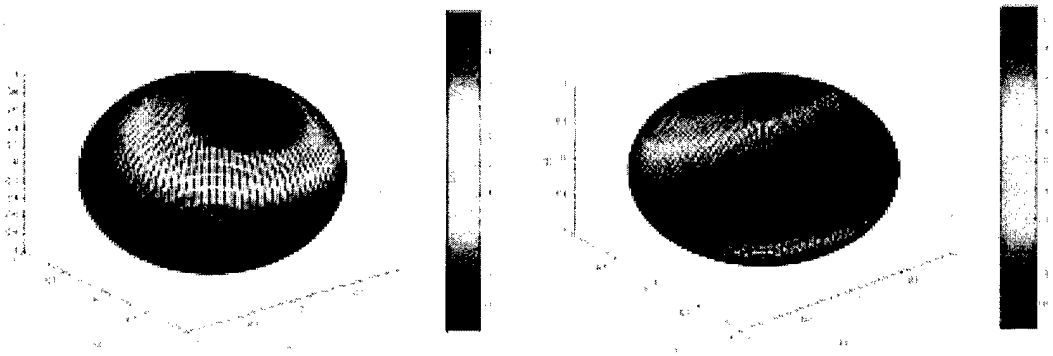

Figure 5. Stokes vector reconstruction error as a function of the incident Stokes vector on the Poincarè sphere. The polarimeter used is a rotating retarder polarimeter that has been optimized to minimize the average error over all possible incident states. The retardance is 110° and the measurement angles are $\{\pm 15.1°, \pm 51.6°\}$. The color scale is labeled in terms of RMS error per square radian of positioning error variance. This theory is only valid for small angles.

The analyses above of SNR and systematic errors were each performed in the absence of the other, i.e. the SNR studies were made with "error free" polarimeters, and the error studies were made in the absence of noise. This raises the obvious question as to how these two types of errors interact. We modeled an active (Mueller matrix) polarimeter and a passive Stokes vector polarimeter on the testbed that had both random positioning errors and detector noise. Both types of errors were controllable, and we found that the balance between the two types of noise affects the "optimum" system design. These experimental results are presented in fig. 6 and fig. 7.

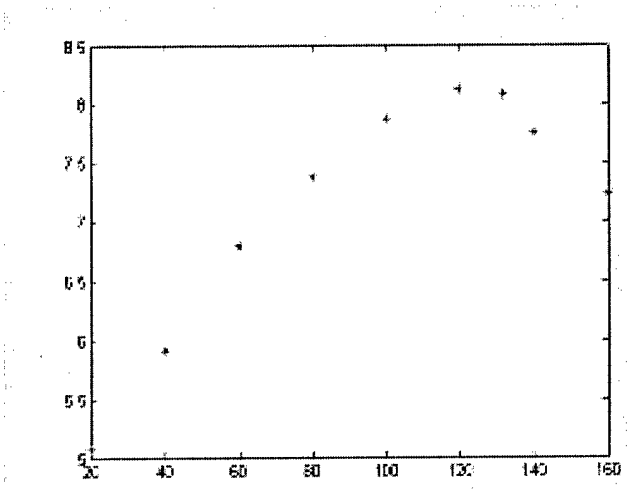

Figure 6. Average Mueller matrix element SNR for a dual rotating retarder polarimeter. The vertical axis shows average SNR over all 16 elements of the Mueller matrix and the horizontal axis shows the value used for the retarders. These data were obtained using 16 measurements, with the angular settings of both the generator and analyzer set to the optimum angles.[8,11] In this experiment, both noise and error were present. The optimum retardance was between that predicted by considering SNR alone (132°)[8,11] and error alone (110°).[11]

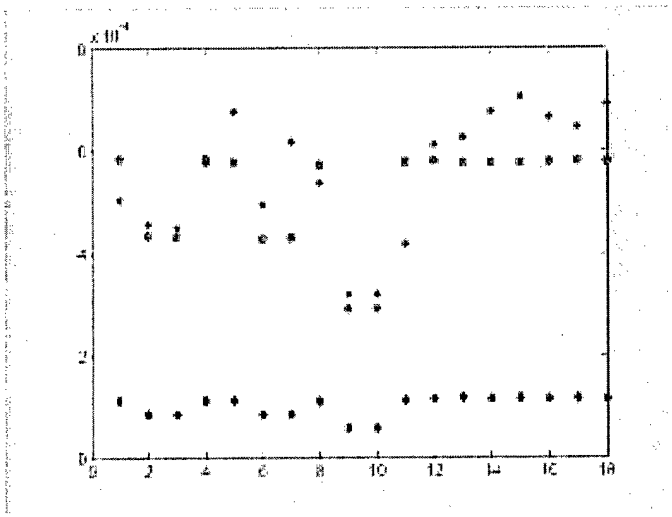

Figure 7. SNR measurements as a function of the input polarization state for a rotating retarder polarimeter. Eighteen different input polarization states including RCP, LCP, eight linear polarization states, and eight elliptical polarization states were tested. The asterisks (∗) show the experimentally measured SNR values. The pink diamonds show the corresponding simulation results assuming only positioning error. The green circles assume an equal amount of positioning error and detector noise error. This is the first observation of the dependence of SNR on input polarization state, and verifies fig. 5.

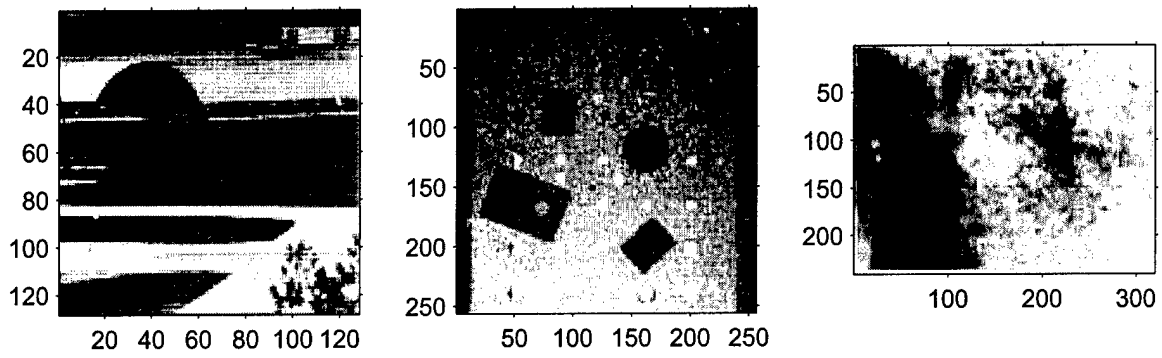

Figure 8. Example images illustrating the nonuniformity-noise phenomenon: (left) an InSb mid-wave FPA, (middle) a HgCdTe long-wave FPA and (right) an uncooled Amorphous-Silicon microbolometer FPA.

4. EXPLORATION OF THE EFFECTS OF FPA NONUNIFORMITY ON POLARIZATION IMAGES

Nonuniformity (NU) noise is one of the key factors that limit the performance of modern focal-plane-array (FPA) sensors in both intensity and polarization imaging applications. NU noise results from the dissimilarities in the photo response and dark current from detector to detector within the array, and it is particularly prevalent in the mid-wave and long-wave infrared (IR) regime. Representative images illustrating the presence of nonuniformity noise obtained for both cryogenically cooled and uncooled cameras are shown in fig. 8. Combating this type of spatial noise is not only essential in thermal imaging and spectral sensing, but also in multi-sensor systems such as polarimeters where NU noise leads to sensor-to-sensor irregularities, which in turn, can severely degrade the performance of linear combination algorithms that produce the final Stokes vector images. What makes the compensation for nonuniformity noise very challenging is the fact that these pixel-to-pixel irregularities slowly drift in time, making a one-time factory calibration ineffective. This drift is a serious problem in array sensors, and in practical systems (including airborne and space-based systems) frequent calibration is necessary to periodically update the nonuniformity correction (NUC) mapping. Additionally, the nonuniformity noise is dependent on the optical spectrum of the target, which we term chromatic nonuniformity. Thus, a NUC map for one target (a panchromatic source, say) may be unsatisfactory for another source (a narrow band source, say). NUC is typically carried out by either a calibration process or a scene-based computational method.

4.1. Effects of FPA NU on Rotating Retarder Systems

A rotating retarder (RR) polarimeter is one of the most common configurations for both imaging and non-imaging polarimeters systems.[14] A rotating retarder system works via the layout presented in fig. 9. A retarder of fixed retardance (often a quarter waveplate - QWP) is rotated in front of a fixed linear polarizer. The image that passes through these polarization optics is then imaged by the *same* focal plane array four different times. Because the NU is the same in each of the four images, we can expect it to have an effect on the reconstructed Stokes parameter images. Fig. 10 shows the

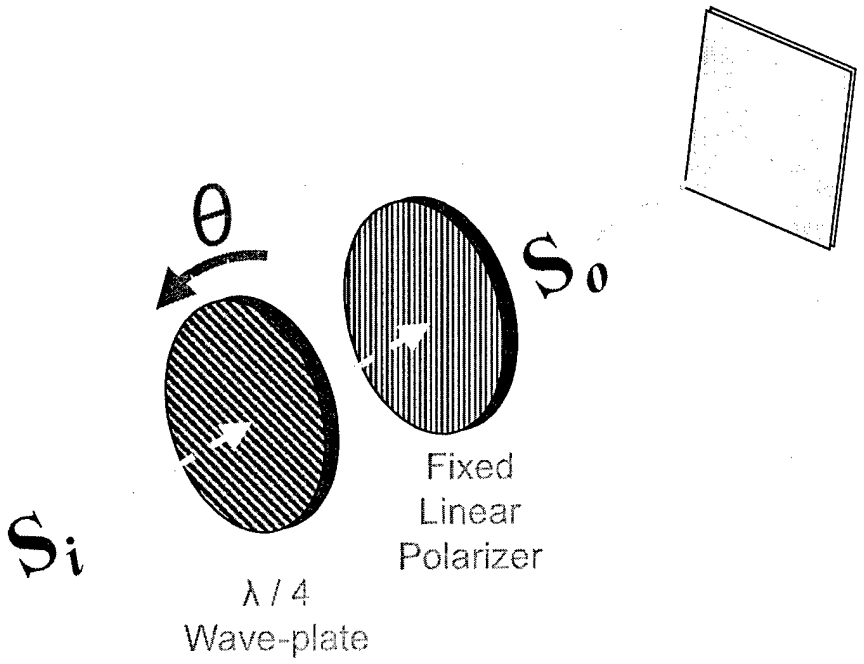

Figure 9. A rotating retarder polarimeter is composed of a rotating retarder of fixed retardance in front of a fixed linear polarimeter.

simulated operation of a RR polarimeter in the presence of bias NU. In the top row, each of the four intensity images (corresponding to the four angular setting of the retarder) are shown corrupted by bias NU with a SNR of 10 dB. What is interesting in this figure is the effect of the bias NU on the resoncstructed Stokes images. The second row shows the four raw Stokes parameters, s_0, s_1, s_2, and s_3. Because s_1, s_2, and s_3 are composed of equal-weighted differences, the bias NU exactly cancels. However, the bias NU is visible in the s_0 image. The third row shows the normalized Stokes images, DOP, s_1/s_0, s_2/s_0, and s_3/s_0. In these images, the bias NU is apparent because they are normalized to s_0, which contains the NU.

Fig. 11 shows comparable results for the case of gain NU. In this set of images, we see that the NU disappears in the normalized images. This effect is due to the fact that gain NU is multiplicative, and has equal weight in the numerator and denomintor in computing the normalized images. Fig. 12 shows what happens in a case with both bias and gain NU, where neither set of images is perfect, and NU correction is needed. Future work will focus on correcting the NU for polarization imagers, and exploring the effects of NU on other classes of polarimeters.

5. CONCLUSIONS

This research effort has focused on two aspects of instrumental errors in polarimeters. The first area includes systematic errors due to misaligned optics, poorly calibrated components, and spatially varying polarization parameters. We have learned how to quantify these error sources, and to understand

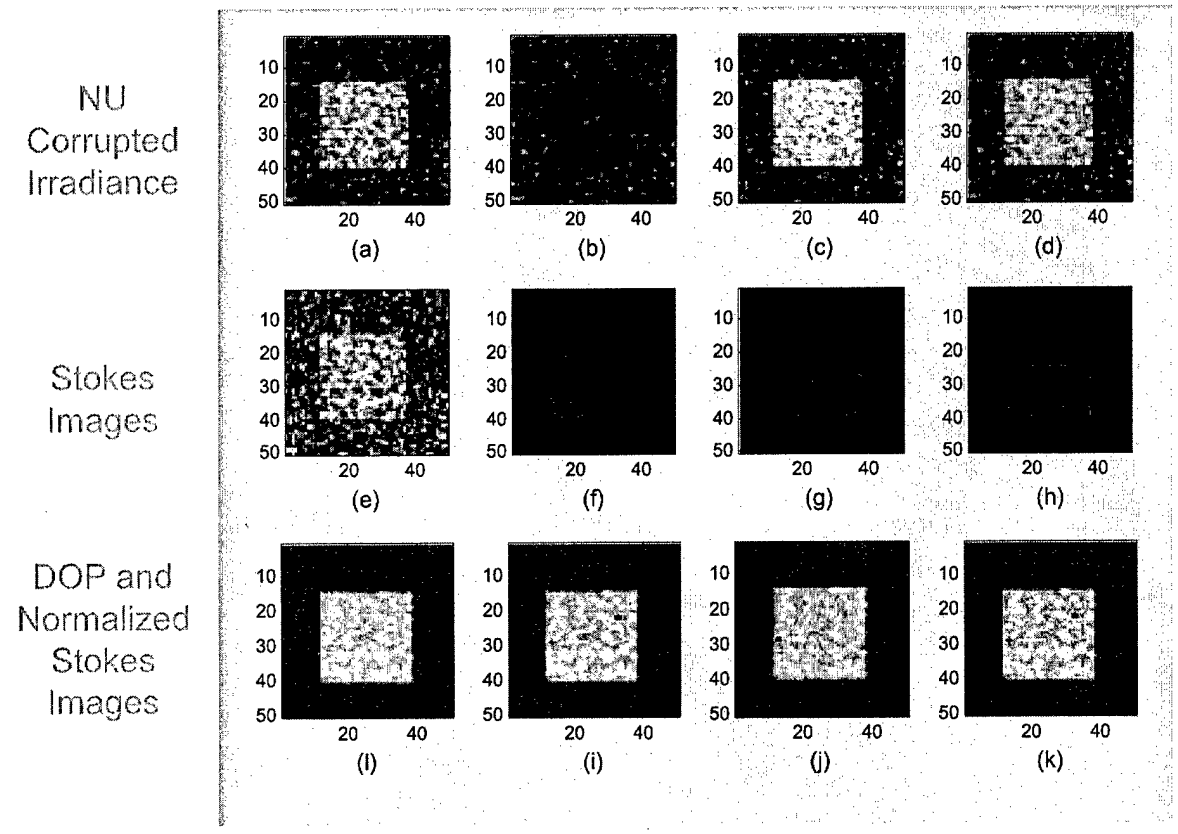

Figure 10. A RR polarimeter operating in the presence of bias NU noise with SNR = 10 dB.

the balance between noise and systematic errors. Our second area of interest has been in the characterization of FPA nonuniformity noise and its effect on imaging polarimeters.

There is still significant work to be done. We have characterized noise sources, but have not yet established reliable methods to mitigate the noise in the final Stokes imagery. Likewise, we have limited ourselves to specific configurations, and need to investigate the performance of other systems.

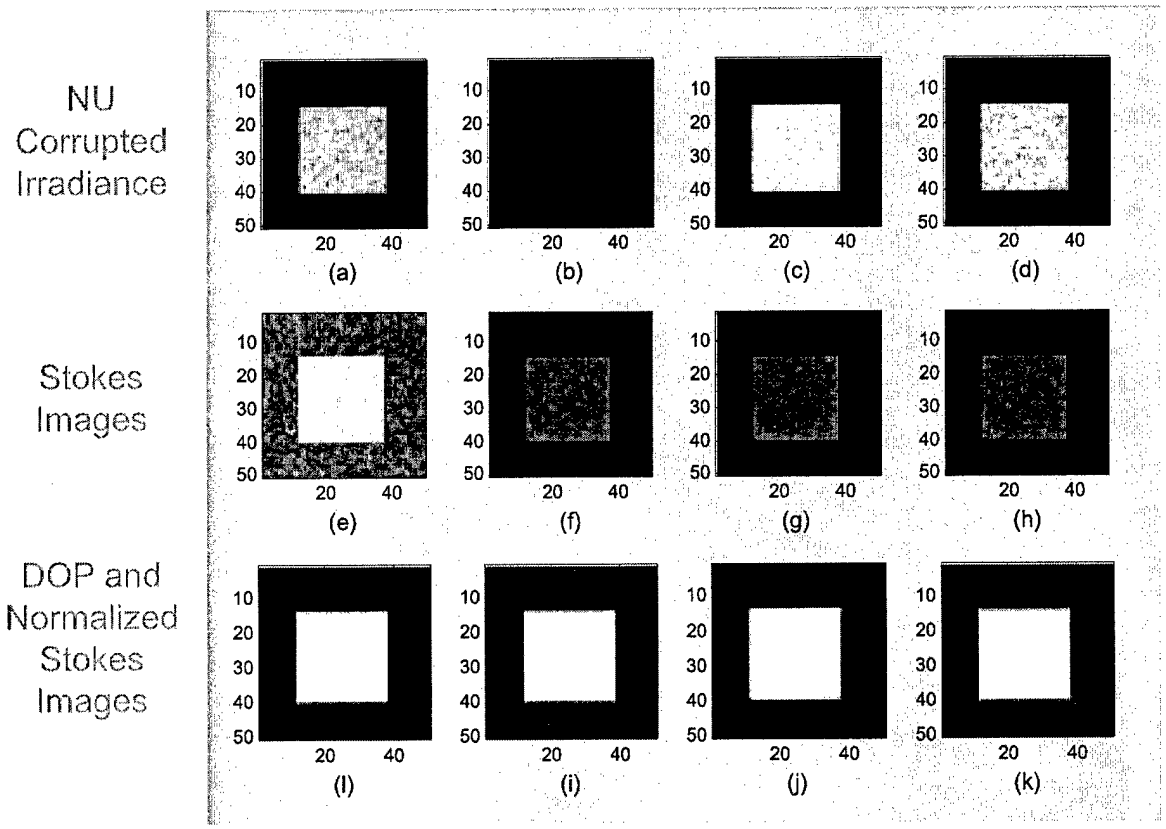

Figure 11. A RR polarimeter operating in the presence of gain NU noise.

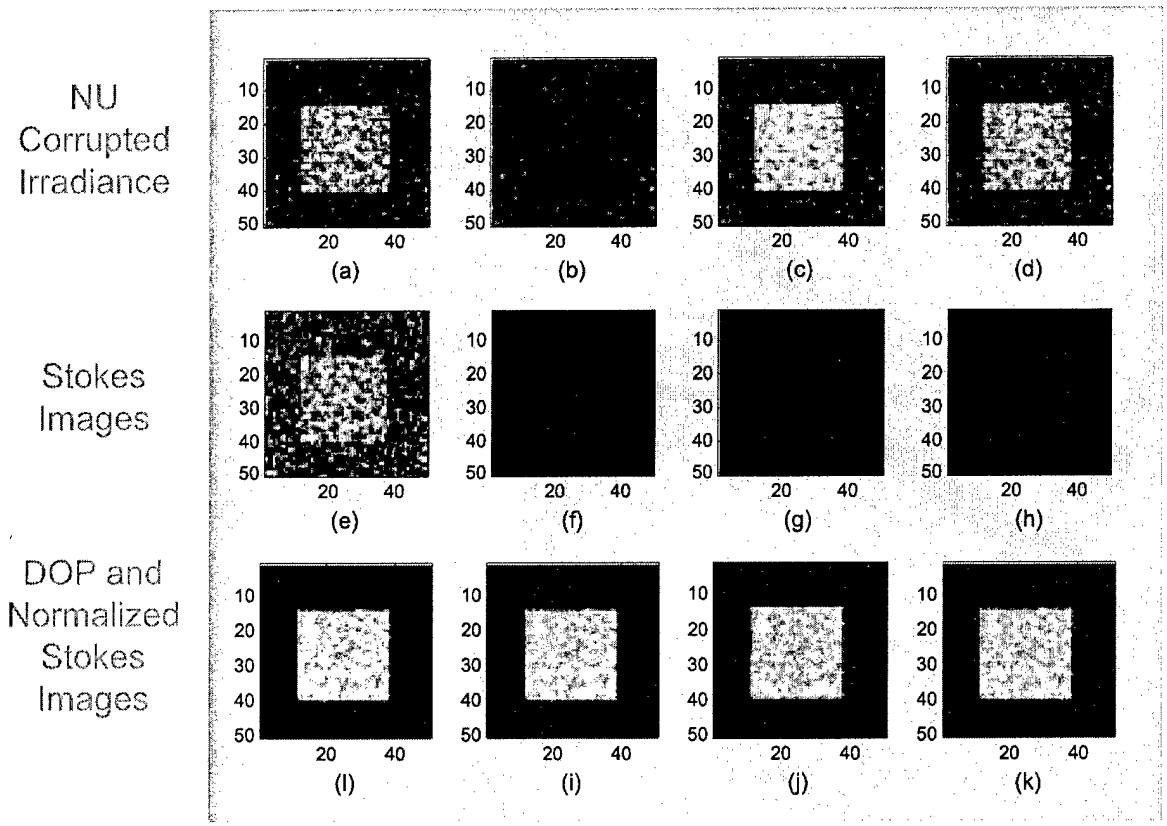

Figure 12. Both bias and gain NU noise are present in these images.

REFERENCES

1. J. S. Tyo, M. P. Rowe, E. N. Pugh, and N. Engheta, "Target detection in optically scattering media by polarization-difference imaging," *Appl. Opt.* **35**, pp. 1855–1870, 1996.
2. T.-W. Nee and S.-M. F. Nee, "Infrared polarization signatures for targets," in *Proceedings of SPIE vol. 2469, Targets and Backgrounds: Characterization and Representation*, pp. 231–241, SPIE, (Bellingham, WA), 1995.
3. L. B. Wolff and T. E. Boult, "Constraining object features using a polarization reflectance model," *IEEE Trans. Patt. Analysis Machine Intell.* **13**, pp. 635–657, 1991.
4. W. G. Egan, W. R. Johnson, and V. S. Whitehead, "Terrestrial polarization imagery obtained fromt he space shuttle: characterization and interpretation," *Appl. Opt.* **30**, pp. 435–442, 1991.
5. L. J. Cheng, M. Hamilton, C. Mahoney, and G. Reyes, "Analysis of aotf hyperspectral imaging," in *Proceedings of SPIE Vol. 2231, Algorithms for Multispectral and Hyperspectral Imagery*, A. Iverson, ed., pp. 158–166, SPIE, (Bellingham, WA), 1994.
6. P. C. Y. Chang, J. G. Walker, K. I. Hopcraft, B. Ablitt, and E. Jakeman, "Polarization discrimination for active imaging in scattering media," *Opt. Commun.* **159**, pp. 1–6, 1999.
7. A. Ambirajan and D. C. Look, "Optimum angles for a polarimeter: part I," *Opt. Eng.* **34**, pp. 1651–1655, 1995.
8. D. S. Sabatke, M. R. Descour, E. Dereniak, W. C. Sweatt, S. A. Kemme, and G. S. Phipps, "Optimization of retardance for a complete Stokes polarimeter," *Opt. Lett.* **25**, pp. 802–804, 2000.
9. J. S. Tyo, "Noise equalization in Stokes parameter images obtained by use of variable retardance polarimeters," *Opt. Lett.* **25**, pp. 1198–2000, 2000.
10. M. H. Smith, "Optimization of a dual-rotating-retarder Mueller matrix polarimeter," *Appl. Opt.* **41**, pp. 2488–2495, 2002.
11. J. S. Tyo, "Design of optimal polarimers: maximization of SNR and minimization of systematic errors," *Appl. Opt.* **41**, pp. 619–630, 2002.
12. D. H. Goldstein and R. A. Chipman, "Error analysis of a Mueller matrix polarimeter," *J. Opt. Soc. Am. A* **7**, pp. 693–700, 1990.
13. M. H. Smith, J. B. Woodruff, and J. D. Howe, "Beam wander considerations in imaging polarimetry," in *Proceedings of SPIE vol. 3754, Polarization Measurement, Analysis, and Remote Sensing II*, D. H. Goldstein and D. B. Chenault, eds., pp. 50–54, SPIE, (Bellingham, WA), 1999.
14. R. A. Chipman, "Polarimetry," in *Handbook of Optics*, M. Bass, ed., vol. 2, ch. 2, McGraw-Hill, 1995.